

MIMO Space-Time Correlation Model for Microcellular Environments

Hamidreza Saligheh Rad and Saeed Gazor
 Department of Electrical and Computer Engineering,
 Queen's University, Kingston, Ontario, K7L 3N6, Canada.
 Tel: (613) 533-6068, Fax: (613) 533-6615,
 Email: radh@ee.queensu.ca

Abstract — In this paper we present a comprehensive cross-correlation model for a Multiple-Input Multiple-Output Rayleigh fading channel in an isotropic scattering environment. The scattering environment is assumed to be a microcellular media with sufficient number of scatterers. This implies uniformly distributed angle of departure and angle of arrival either at the transmitter or at the receiver. Simple and reasonable assumptions are made for various relevant physical parameters, such as exponential or normal time-delay distribution and uniform phase change in the receiving waveform. A novel method of modeling is suggested to consider a geometry for the local scatterers. This approach establishes a mathematical relation between the time-delay and the channel gain associated to each dominant propagation path, and uses appropriate probability density function (pdf) for the time-delay profile. This flexible method allows us to characterize a wide range of propagation environments. Cross-correlation function between channels appears to be a multiplication of two Bessel functions, and two other multiplicative terms. Bessel functions represent the Doppler effect, the carrier frequencies, and the spatial separation, either at the transmitter or at the receiver. The effect of the carrier frequencies also appears on the other terms. Interestingly, the last two terms are $\eta/2$ -order derivative of the moment generating function of the delay profile at two carrier frequencies, respectively, where η is the environment pathloss exponent. Overall, the model has a closed form and is a generalization of the Clark model.

I. INTRODUCTION

Multiple-Input Multiple-Output (MIMO) communication systems hold considerable promise for providing high data rates [1]. To design a real MIMO wireless system, and to predict its performance, it is necessary to have accurate MIMO wireless channel models. Hence, simple and reliable models for the underlying MIMO channels are necessary to analyze the impact of the random multipath fading channel on the performance of ST solutions [2]. Statistical behavior of the time-varying Channel Impulse Response (CIR) is a key method to characterize MIMO communication systems [1–5, 7]. On the other hand, in most environments the communication channel response is the superposition of responses of a large number of propagation paths. This fact, along with the central limit theorem, suggests an asymptotically zero-mean Gaussian random process for the channel; therefore, such a random process is often characterized by its second-order statistics, i.e., cross-correlation function [16]. In this paper a physical model is presented based on the calculation of these statistics.

Some interesting physical models based on cross-correlation function are discussed in the literature [1–4]. The one-ring model first employed by Jakes [15] is extended in [1] for MIMO channels. This extended model is appropriate in the urban macrocell environments, where the BS is elevated and seldom obstructed. In [4], another extension of the traditional Clarks/Jakes' model (see [15] and [7]) is proposed for frequency flat fading process in a land macrocell mobile radio environment. This work develops a ST correlation function using a ring of scatterers around the mobile unit. Abdi and Kaveh in [2] propose a ST cross-correlation function for a MIMO frequency nonselective Ricean fading channel, assuming a one-ring of scatterers around the Mobile Station (MS). In this model as an example of an outdoor macrocell environment, a nonuniform probability density function (pdf) is suggested for the Direction Of Arrival (DOA) around the user, mod-

eled by the von Mises distribution [2]. Kalkan and Clarke suggest a model to predict the BS signal statistics in the urban macrocell environments where there is no scattering around the BS [3]. Using this model, the correlation for the envelope of channels is derived for the case of hybrid space-frequency diversity reception. All of mentioned models consider one-ring of scatterers with different statistical assumptions on physical parameters.

In this paper we derive a closed-form, easy-to-use, and mathematically tractable expression for the ST cross-correlation function between correlated links of a Rayleigh wireless channel with Multiple-Transmit Multiple-Receive antennas. A novel method of modeling, called free-geometry scatterers, is suggested to consider the spatial distribution for the local scatterers. This approach establishes a mathematical relation between the time-varying delay and the correlated channel gain associated with each dominant propagation path, and uses appropriate statistical distributions for physical parameters such as the time-delay. This method gives us the flexibility to characterize different propagation environments: microcell or macrocell, flat-fading or frequency-selective. In fact, this delay-gain expression, along with the appropriate statistical distributions for the time-delay and the angle spread, plays the role of the geometry of scatterers in the modeling process [5]. Each dominant path is associated with a path gain and a path phase change. The path gain represents pathloss and fading effects of the propagation waves along the path. The path phase change represents the contribution of the path on the phase of the received signal. This simple physical model considers a homogenous¹ scattering environment with a large number of surrounding local isotropic² scatterers.

Waves propagated in the environment are assumed to be planar. This assumption is possible because the distance between the BS and the MS is large enough. The planar wave propagation in a homogenous environment is a reciprocal phenomenon; thus, the proposed model can be used in both uplink and downlink channel modeling. In addition, we take into account the temporal information of the propagation media, as well as the effect of the multiple propagation paths. In other words, this model describes general statistical characteristics of the Rayleigh channel as a function of space, time, and frequency. Overall, the proposed model is efficient for both analytical analysis and simulations purposes of MIMO wireless systems [9, 10]. An extension of the model for a three-dimensional (3D) propagation scenario is also given in [6].

The rest of this paper is organized as follows. Notations and assumptions of a MIMO channel model for the free-geometry scattering method are introduced in Section II. The new space-time-frequency cross-correlation function is derived in Section III. Some simulation results and discussions of the behavior of the model are proposed in Section IV. The results describe the effect of different assumptions on the modeling procedure. The discussion elements that occur throughout this paper are brought together as concluding remarks in Section V.

II. MIMO RAYLEIGH FADING CHANNEL

Figure 1 shows a pair of BS-MS antennas from a multielement antenna system in a two-dimensional (2-D) propagation environment. Throughout this paper, the following notations are used where the superscripts

¹By homogenous propagation media, we mean an environment with identical (homonized) random physical features in all directions in space.

²An isotropic scatterer is a very small scatterer compared to the wavelength of the carrier frequency. Such a scatterer acts as a point source [8].

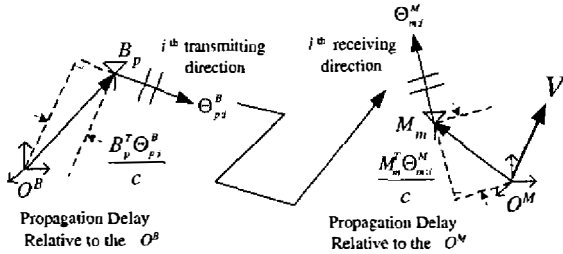


Fig. 1. p^{th} antenna of the BS and m^{th} antenna of the MS in their local coordinate axis. The time-delay of the i^{th} propagating waveform to the MS has three different components: two small relative propagation delays and one major distance delay.

B and M indicate variables at the BS and MS sides respectively:

O^B	BS coordinate,
O^M	MS coordinate,
ω	Carrier frequency,
$h_{mp}(t, \omega)$	CIR between p^{th} BS and m^{th} MS antenna elements,
n^B	Number of BS antenna elements,
n^M	Number of MS antenna elements,
B_p	p^{th} antenna element on the BS side relative to O^B ,
M_m	m^{th} antenna element on the MS side relative to O^M ,
V	MS speed vector,
c	Wave propagation velocity,
Θ_i^B	The unity vector pointing to the Direction of Departure (DOD) of the i^{th} dominant path wave from the BS,
Θ_i^M	The unity vector pointing to the DOA of the i^{th} dominant path wave from the MS,
I	Number of total dominant paths,
$\tau_{p,m;i}$	Delay between p^{th} BS and m^{th} MS antenna elements via i^{th} dominant path,
$g_{p,m;i}$	Gain between p^{th} BS and m^{th} MS antenna elements via the i^{th} dominant path, approximated by g_i ,
ϕ_i	Phase contribution along the i^{th} dominant path,
θ	Uniform distribution parameter for phase change,
ω_i	Shifted frequency by the Doppler phenomenon for the i^{th} dominant path,
β_i	Fast fading factor for the i^{th} path,
η	Pathloss exponent,
σ	Variance of the time-delay τ_i ,
$\bar{\tau}$	Mean of the time-delay τ_i .

In Figure 1 antenna elements are arbitrarily located at MS and BS, around their local coordinates. O^B and O^M . All antennas are assumed to be omnidirectional and are addressed by position vectors with respect to their local coordinates. BS and MS have n^B and n^M antenna elements respectively. Each antenna receives the signal through the media via a large number of propagating paths with uniform DODs and DOAs over $[0, 2\pi)$, since the MS and the BS are assumed to have almost the same height [13]. The distance between MS and BS coordinates is considerably larger than the space between the antenna elements which is defined in the mean value of the time-delay distribution. This implies a planar wave propagation environment [13, Page 75]. Hence, as long as there is no scattering on the waveform traveling between two antenna elements, this is reasonable to assume that DODs and DOAs are the same for all the antenna elements in the corresponding station³. Overall, the propagation media is considered to be a rich scattering microcellular environment. We assume that there is no LOS which can be treated as one of these propagation paths and can be deterministically modeled [2]. Notations Θ_i^B and Θ_i^M represent DOD and DOA unity vectors of the i^{th} path at BS and MS respectively (see Figure 1). The vector V represents the MS mobility on a horizontal plane. This

³Planar wave propagation in a homogenous environment is a reciprocal phenomenon [18].

assumption is made to characterize the time selectivity (temporal variation behavior) or the "time coherence" of the channel [13, Page 30-32].

A solution basis for Maxwell's equations is to break down the received waveform into a linear combination of an appropriate set of elementary functions [13], e.g., the set of plane waves [13, 17]. Planar waves emitted from the array element B_p travel over several propagation paths with different lengths. We assume that the waves are scattered in the propagation media and reach the MS via a number of dominant paths from different directions. The following expression describes the CIR of such a propagation scenario,

$$h_{mp}(t, \omega) = \frac{1}{\sqrt{I}} \sum_{i=1}^I g_{p,m;i} \exp(j\phi_i + j\omega_i t - j\omega\tau_{p,m;i}), \quad (1)$$

where I is the number of dominant paths resulting from scattering, $\tau_{p,m;i}$ is the real time-delay over i^{th} path, and $g_{p,m;i}$ is the real gain of the i^{th} dominant path between B_p and M_m . The gain, $g_{p,m;i}$, is a function of the time-delay and the fast fading factor [2,5]. The frequency of the i^{th} received waveform is denoted by $\omega_i \triangleq \omega(1 + \frac{V^T \Theta_i^M}{c})$, where ω is the carrier frequency and $(\frac{V^T \Theta_i^M}{c})$ is the Doppler spread factor. Notation ϕ_i denotes the phase change of the signal along the i^{th} path. The term $1/\sqrt{I}$ is introduced to avoid any divergence in the summation by retaining a constant energy random process, i.e., to guarantee $I^{-1} \sum_{i=1}^I E[g_i^2] \rightarrow 1$ as $I \rightarrow \infty$ [16].

In this paper, we make the following statistical assumptions:

- A1) Statistical distribution of DODs and DOAs are all uniform. This is possible by the assumption of a homogenous rich scattering environment with a planar wave propagation between BS and MS [13]. In addition, we assume that DOAs and DODs are independent from each other and from time-delays, $\tau_{p,m;i} \in [1-4]$.
- A2) In this model the phase contribution of surrounding scatterers are taken into account by a random phase change parameter, ϕ_i . This random phase plays a significant role in the resulting model. In order to consider different types of scatterers, we model the phase change by a uniform pdf with an adjusting parameter as: $p_\phi(\phi) \sim U[0, 2\theta)$; $0 \leq \theta < \pi$, where θ is called the softness factor of the environment. This parameter characterizes the effect of the environment on the phase change; e.g., a hard scatterer has no contribution on the phase of the reflecting waveform, while a soft scatterer introduces a phase change. More specifically, two special extreme cases are:
 - A2a. Hard environment $\theta = 0$: The phase change is considered to be zero, i.e., all reflecting scatterers are assumed to be hard [8].
 - A2b. $p_\phi(\phi) \sim U[0, 2\pi)$: In this case, random variations of the phase change is at the maximum. This distribution is suitable for those environments in which a typical radio wave travels long distances, usually the distance of hundreds or thousands of wavelengths, and hits so many scatterers before reaching the receiver [13]. Obviously, one can assume more realistic, but more complex phase models [11].
- A3) We decompose the i^{th} path propagation delay, $\tau_{p,m;i}$, into three components: one major distance delay, and two relative propagation delays with respect to local coordinates across BS and MS antenna arrays. This can be written in the following form:

$$\tau_{p,m;i} = \tau_i - (\tau_{p;i}^B + \tau_{m;i}^M), \quad (2a)$$

$$\tau_{p;i}^B \triangleq \frac{B_p^T \Theta_i^B}{c}, \quad (2b)$$

$$\tau_{m;i}^M \triangleq \frac{M_m^T \Theta_i^M}{c}, \quad (2c)$$

where τ_i represents distance delay between O^B and O^M , and $\tau_{p;i}^B$ and $\tau_{m;i}^M$ represent relative propagation delays from antenna

elements, B_p or M_m , to corresponding coordinates, O^B or O^M respectively [5]. We consider two common distributions for distance delays, τ_i , in order to be able to compare their effect on the model. In one case, time-delays are assumed to be independent identically distributed (i.i.d.) Gaussian random variables, $\tau_i \sim \mathcal{N}(\bar{\tau}, \sigma) = \frac{1}{\sqrt{2\pi}\sigma} e^{-\frac{x-\bar{\tau}}{2\sigma^2}}$. The second case, as is used in [3], assumes i.i.d. Exponential distributions for time-delays, τ_i . For the sake of comparison, the distribution of the exponential case is considered to be $\tau_i \sim \frac{1}{\sigma} e^{-\frac{x-\bar{\tau}}{\sigma}}$, $\forall x \geq \bar{\tau} - \sigma$. In both cases, the average time-delay, $\bar{\tau}$, is related to the propagation distance and σ is the variance of the propagation delay. The moment generating functions for these two cases are given respectively by [16, page 153]:

$$\text{Normal: } \Phi_{\tau}(s) = e^{\bar{\tau}s + \sigma^2 s^2 / 2}, \quad (3a)$$

$$\text{Exponential: } \Phi_{\tau}(s) = \frac{e^{-(\bar{\tau}-\sigma)s}}{1-\sigma s}. \quad (3b)$$

- A4) Path gain, $g_{p,m,i}$, and propagation delay, $\tau_{p,m,i}$, are two random parameters as functions of path length; therefore, they are dependent. The following relation, which is justified by experimental measurements [15], is used to describe this interaction [5]:

$$g_{p,m,i} \triangleq \beta_i \sqrt{P(\tau_{p,m,i})}, \quad (4)$$

where $P(\tau_{p,m,i})$ is the average pathloss power, and β_i is called the fast fading factor [17,18]. The fast fading factor is assumed to be stationary, independent of the time-delay, $\tau_{p,m,i}$, and a time-invariant random process for a stationary time-varying channel. The effect of slow fading is also taken into account in the log-normal component [17]. By experimental measurements, it has been found that the dependency of the pathloss on the time-delay, $\tau_{p,m,i}$, is characterized by [14]

$$P(\tau_{p,m,i}) \triangleq \left(\frac{\tau_{p,m,i}}{\bar{\tau}}\right)^{\eta} P_0, \quad (5)$$

where, η is called pathloss exponent, and P_0 is a constant. Depending on the characteristics of the propagation media, the pathloss exponent is usually measured between 2 and 6 [5, 14]. From (5), (2a) and the obvious fact that $|\tau_i| \gg \max\{|\tau_{p,i}^B|, |\tau_{m,i}^M|\}$, we approximate $P(\tau_{p,m,i}) \simeq P(\tau_i)$ for all BS and MS antennas as:

$$g_{p,m,i} \simeq g_i = \beta_i \left(\frac{\tau_i}{\bar{\tau}}\right)^{\frac{\eta}{2}} \sqrt{P_0}. \quad (6)$$

- A5) It is assumed that random phase change, ϕ_i , is independent from channel gain, time-delay, and fast fading factor, β_i .

III. A NEW SPACE-TIME CROSS-CORRELATION FUNCTION

Using established assumptions in the previous section, we derive a closed-form expression for the ST cross-correlation function between the CIRs of two arbitrary communication links, $h_{mp}(t_1, \omega_1)$ and $h_{nq}(t_2, \omega_2)$. This correlation function is denoted by,

$$R_{mp,nq}(t_1, t_2; \omega_1, \omega_2) \triangleq E[h_{mp}(t_1, \omega_1) h_{nq}^*(t_2, \omega_2)], \quad (7)$$

and is a function of sampling times (t_1, t_2), carrier frequencies (ω_1, ω_2), and antenna elements ($m, p; n, q$). This second-order statistics provides essential information for the random process describing the propagation behavior of the MIMO communication channel.

By replacing (1) and (2) in (7), the ST correlation function $R_{mp,nq}(t_1, t_2; \omega_1, \omega_2)$ is written as follows:

$$E\left[\frac{1}{I} \sum_{i_1=1}^I \sum_{i_2=1}^I g_{p,m,i_1} g_{q,n,i_2} \exp(j(\phi_{i_1} - \phi_{i_2})) \Psi_1 \Psi_2^*\right], \quad (8a)$$

where,

$$\Psi_1 \triangleq e^{j\omega_{i_1} t_1 - j\omega_{i_1}(\tau_{i_1} - \frac{d^T \Theta_{i_1}^B + M_m^T \Theta_{i_1}^M}{c})}, \quad (8b)$$

$$\Psi_2 \triangleq e^{j\omega_{i_2} t_2 - j\omega_{i_2}(\tau_{i_2} - \frac{d^T \Theta_{i_2}^B + M_n^T \Theta_{i_2}^M}{c})}, \quad (8c)$$

and $\omega_{i_1} \triangleq \omega_1(1 + \frac{v^T \Theta_{i_1}^M}{c})$ and $\omega_{i_2} \triangleq \omega_2(1 + \frac{v^T \Theta_{i_2}^M}{c})$. Relative location of the antenna elements on the MS side are assumed to be constant with respect to each other. This assumption also applies for the BS. The motion of the mobile unit is expressed by the relative motion of the BS and the MS coordinates. In fact, motion of a MS with a constant speed results in a Doppler spectrum that is usually modeled by a Bessel function for the Single-Input Single-Output (SISO) scenario [7]. In a planar wave propagation environment, we assume that DODs: $\Theta_{i_1}^B$ and $\Theta_{i_2}^B$, and DOAs: $\Theta_{i_1}^M$ and $\Theta_{i_2}^M$, do not depend on antenna indices. There is no more scattering when the wave travels between antenna elements in both MS and BS; therefore, phase changes of dominant paths corresponding to different MIMO channels are equal.

By regrouping dependent and independent random variables in (8a), using Assumptions A1-4, and doing some manipulations, $R_{mp,nq}(t_1, t_2; \omega_1, \omega_2)$ is decomposed into four components as follows

$$\frac{1}{I} \sum_{i_1, i_2=1}^I E[g_{i_1} g_{i_2} e^{j(\omega_2 \tau_{i_2} - \omega_1 \tau_{i_1})}] E[e^{j(\phi_{i_1} - \phi_{i_2})}] J_0\left(\frac{d^B}{c}\right) J_0\left(\frac{d^M}{c}\right) \quad (9a)$$

where

$$d^B \triangleq |\omega_1 B_p - \omega_2 B_q|, \quad (9b)$$

$$d^M \triangleq |(\omega_1 t_1 - \omega_2 t_2) V + (\omega_1 M_m - \omega_2 M_n)|, \quad (9c)$$

$J_0(z) \triangleq \frac{1}{2\pi} \int_0^{2\pi} e^{jz \cos \alpha} d\alpha$, and the amplitude of a complex vector is denoted by $|\cdot|$. Parameters d^B and d^M represent shifted distances at BS and MS respectively. Greater d^B and d^M often result in less ST correlation because of the form of the Bessel function. Parameters d^B and d^M contain spatial, temporal, and frequency separation between $h_{m2}(t_1, \omega_1)$ and $h_{nq}(t_2, \omega_2)$.

One should note that correlations appear in a multiplicative form defined by two Bessel functions. This closed-form is easy to use and accurate enough for different analytical and simulation purposes [9,10]. In addition, the simplicity of this form is easy to understand, but it is sufficiently comprehensive to describe the MIMO propagation media for advanced educational objectives.

Remark 1: In a fixed carrier frequency, $\omega_1 = \omega_2$, the proposed cross-correlation function depends on the time difference, $t_1 - t_2$ [7,15]. This implies that the suggested scenario for MIMO channel modeling offers a stationary random process in a narrowband communication system.

Replacing (6) in (9a), using Assumption 5, and using the moment generating functions of time-delays, we get

$$R_{mp,nq}(t_1, t_2; \omega_1, \omega_2) = J_0\left(\frac{d^B}{c}\right) J_0\left(\frac{d^M}{c}\right) \Phi_{\tau}^{\left(\frac{\eta}{2}\right)}(-j\omega_1) \Phi_{\tau}^{\left(\frac{\eta}{2}\right)}(j\omega_2) \times \frac{P_0}{\bar{\tau}^{\eta}} \sum_{i_1=1}^I \sum_{i_2=1}^I E[\beta_{i_1} \beta_{i_2}] E[\exp(j(\phi_{i_1} - \phi_{i_2}))], \quad (10)$$

where $\Phi_{\tau}^{\left(\frac{\eta}{2}\right)}(s)$ is obtained by $\left(\frac{\eta}{2}\right)^{\text{th}}$ -times differentiating the moment generating function, $\Phi_{\tau}(s)$ [16, Page 153]. We assume that $\frac{\eta}{2}$ is a positive integer number, otherwise partial differentiating or other methods are required to evaluate the above expression. The appropriate value for the pathloss is $\eta = 2$ for free propagation environments, $\eta = 4$ for rural environments, and $\eta = 6$ for crowded urban environments [17, 18]. In this relation the effect of slow fading is taken into account

in the log-normal component [17], while the fast fading component for each path is assumed to be a time-invariant complex random process, β_i . This random process is often considered to be Rayleigh distributed for wireless applications [17, 18]. Phase changes are assumed to be i.i.d. uniform random processes (see Assumption A2); therefore,

$$E[\exp(j(\phi_{i_1} - \phi_{i_2}))] = \begin{cases} 1 & i_1 = i_2, \\ \Phi_{\phi_{i_1}}(j)\Phi_{\phi_{i_2}}(-j) & i_1 \neq i_2, \end{cases} \quad (11a)$$

where the moment generating function of the phase change is,

$$\Phi_{\phi_i}(s) = \frac{e^{s\theta} - e^{-s\theta}}{2s\theta}. \quad (11b)$$

Substituting (11) in (10), for $R_{mp,nq}(t_1, t_2; \omega_1, \omega_2)$, we get

$$J_0\left(\frac{d^B}{c}\right)J_0\left(\frac{d^M}{c}\right)\Phi_{\tau}^{(\frac{\eta}{2})}(-j\omega_1)\Phi_{\tau}^{(\frac{\eta}{2})}(j\omega_2) \quad (12)$$

$$\times \frac{P_o}{\bar{\tau}^{\eta} I} \left(\sum_{i=1}^I E[\beta_i^2] + \left(\frac{\sin \theta}{\theta}\right)^2 \sum_{\substack{i_1, i_2=1 \\ i_1 \neq i_2}}^I E[\beta_{i_1}\beta_{i_2}] \right).$$

Remark 2: Only the last term in (12) depends on the fast fading gains β_i and softness factor θ . This term is also independent of t_1, t_2, ω_1 and ω_2 . Therefore, the shape of the correlation function, $\frac{R_{mp,nq}(t_1, t_2; \omega_1, \omega_2)}{R_{mp,nq}(t_1, t_1; \omega_1, \omega_1)}$ is independent of the fast fading gains β_i , softness factor θ , and P_o . The effect of all these parameters appears as a constant power gain.

Remark 3: The second line in (12) represents a constant gain in the channel model and also represents the effect of fast fading factors, β_i , softness factor, θ , and P_o . As all $\{\beta_i\}_{i=1}^I$ are positive real numbers, it is seen that this term takes its maximum at $\theta = 0$; therefore, a hard environment produces the maximum correlation in the communication. This constant gain, which plays an important role in the communication performance, is determined by following limited statistics: $\theta, \sum_i E[\beta_i^2], E[\sum_i \beta_i^2], P_o$ and I . Fast fading factors, β_i , are often assumed to be Rayleigh distributed [18], and can be approximated by some simplifying assumptions based on the physical characteristics of the propagation media [2, 5].

In Assumption A3 we consider two distributions for the delay profile, i.e., exponential distribution and normal distribution. Differentiating the moment generating functions (3a) of these distributions ($\frac{\eta}{2}$)-times with respect to s results in $\Phi_{\tau}^{(\frac{\eta}{2})}(s)$ for exponential and normal distributions respectively, as follows:

$$e^{s(\bar{\tau}-\sigma)} \sum_{l=0}^{\frac{\eta}{2}} \frac{(\frac{\eta}{2})!}{(\frac{\eta}{2}-l)!} \frac{\sigma^l (\bar{\tau}-\sigma)^{\frac{\eta}{2}-l}}{(1-\sigma s)^{l+1}}, \quad (13a)$$

$$\begin{cases} e^{s\bar{\tau}+s^2\sigma^2/2(\bar{\tau}+s\sigma^2)}, & \text{if } \eta = 2, \\ e^{s\bar{\tau}+s^2\sigma^2/2((\bar{\tau}+s\sigma^2)^2+\sigma^2)}, & \text{if } \eta = 4, \\ e^{s\bar{\tau}+s^2\sigma^2/2((\bar{\tau}+s\sigma^2)^3+3\sigma^2(\bar{\tau}+s\sigma^2))}, & \text{if } \eta = 6. \end{cases} \quad (13b)$$

Using (13) and from (12), $\Phi_{\tau}^{(\frac{\eta}{2})}(-j\omega_1)\Phi_{\tau}^{(\frac{\eta}{2})}(j\omega_2)$ is calculated for exponential and normal distributions.

Remark 4: The dependency of $R_{mp,nq}(t_1, t_2; \omega_1, \omega_2)$ on the carrier frequencies, ω_1, ω_2 via d^B, d^M or $\Phi_{\tau}^{(\frac{\eta}{2})}(-j\omega_1)\Phi_{\tau}^{(\frac{\eta}{2})}(j\omega_2)$, shows that the correlation decreases when these frequencies or their differences, increase. This result is consistent with some other literature proposed for some different propagation environments [4].

IV. NUMERICAL ILLUSTRATIONS

The unit for the antenna spacing is half of the carrier wavelength, $\frac{\lambda}{2} \triangleq \frac{c\pi}{\omega}$.

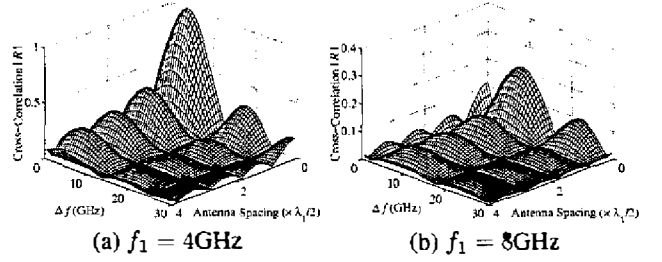


Fig. 2. **Spatial-Frequency selectivity:** Cross-correlation function with respect to the antenna spacing for different frequency offsets, $\Delta f \triangleq f_2 - f_1$: Using Exponential delay profile with mean, $\bar{\tau} = 2\mu\text{sec}$, and variance, $\sigma = 100\text{psec}$, the mobile speed, $V = 50\text{Km/h}$, $t_1 = t_2 = 0$, pathloss exponent, $\eta = 2$, $M_m = 2(1-j)\text{cm}$, $M_n = (1+j)\text{cm}$, $B_p = k\lambda_1/2$, $B_q = 0\text{cm}$, where $k \in [0, 4]$: a) $f_1 = 4\text{GHz}$, b) $f_1 = 8\text{GHz}$.

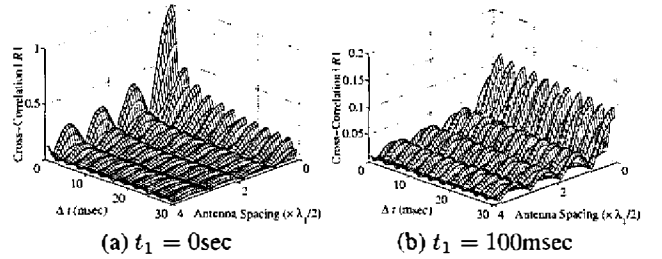


Fig. 3. **Spatial-Temporal selectivity; Non-Stationary case:** Cross-correlation function with respect to antenna spacing for different time offsets, $\Delta t \triangleq t_2 - t_1$, Using exponential delay profile with mean, $\bar{\tau} = 2\mu\text{sec}$, and variance, $\sigma = 100\text{psec}$, the mobile speed, $V = 50\text{Km/h}$, $f_1 = 1, f_2 = 2\text{GHz}$, pathloss exponent, $\eta = 2$, $M_m = 2(1-j)\text{cm}$, $M_n = (1+j)\text{cm}$, $B_p = k\lambda_1/2$, $B_q = 0\text{cm}$, where $k \in [0, 4]$: a) $t_1 = 0\text{sec}$, b) $t_1 = 100\text{msec}$.

In what follows, we use the exponential distribution with a constant mean, $\bar{\tau} = 2\mu\text{sec}$, and variance, $\sigma = 100\text{psec}$ [12, 18]. This profile is selected because it is the most common one used in the literature.

In Figure 2 normalized cross-correlation, $\frac{R_{mp,nq}(t_1, t_2; \omega_1, \omega_2)}{R_{mp,nq}(t_1, t_1; \omega_1, \omega_1)}$, are plotted as a function of the MS antenna spacing and carrier frequency offsets, $\Delta f \triangleq f_2 - f_1$, where $\omega_i = 2\pi f_i$ and f_1 is constant either at 4GHz or at 8GHz. From this figure, it is apparent that the correlation decreases as the difference of carrier frequencies, Δf , increases. This decrease results from the form of the Bessel functions and the term produced from the delay profile moment. We note that (9) represents a non-stationary random process if the carrier frequencies are not equal.

Figure 3 shows joint spatial-temporal selectivity, i.e., the cross-correlation is depicted as a function of $\Delta t = t_2 - t_1$, where t_1 and carrier frequencies, $f_1 = 1\text{GHz}$ and $f_2 = 2\text{GHz}$ are constant. Comparing Figures 3a and 3b, we observe the non-stationary behavior of the MIMO channel. These figures also reveal the fact that the correlation decreases as the antenna spacing increases. In the particular case in which carrier frequencies are equal, the correlation function represents a stationary random process; only a function of the time difference $t_1 - t_2$. This result is in agreement with other results available for stationary models in the literature [1–5].

Figure 4 illustrates the two dimensional spatial selectivity, i.e., the correlation function is plotted as a function of variations of antenna spacing both at the BS and the MS. In this figure we observe the effect of oscillations of Bessel functions in both dimensions. Comparing Figures 4a and 4b shows the non-stationary effect of the time index.

Here we investigate the effect of different scattering environments: free space, rural, and crowded urban propagation environments that are characterized by $\eta = 2, 4$ and 6 [18], respectively. Results are depicted

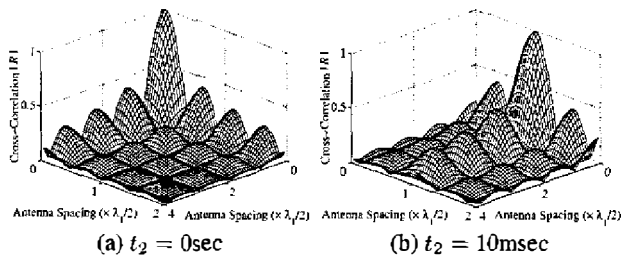


Fig. 4. **Spatial selectivity:** Cross-correlation function with respect to antenna spacing on both BS and MS for different time index, t_2 , when $t_1 = 0$ sec. Using exponential delay profile with mean, $\bar{\tau} = 2\mu\text{sec}$. and variance, $\sigma = 100\text{psec}$, the mobile speed, $V = 50\text{Km/h}$, $f_1 = f_2 = 1\text{GHz}$, pathloss exponent, $\eta = 2$, $M_m = k_1\lambda_1/2$, $M_n = (1+j)\text{cm}$, $B_p = k_2\lambda_1/2$, $B_q = 0\text{cm}$, where $k_1 \in [0, 2]$ and $k_2 \in [0, 4]$: a) $t_2 = 0$ sec, b) $t_2 = 10\text{msec}$.

in Figure 5 for two before-mentioned time-delay profiles. A strong relation between the pathloss and the excess delay spread is reported in the literature [12, 18]; therefore, the amount of the time-delay variance in this figure is appropriately adjusted for each new propagation environment. This figure shows that the model introduces less communication gain when the scattering phenomenon in the environment produces a wider range of time-delay values. The exponential delay distribution provides stronger communication links rather than the normal delay profile. For a given delay profile, the pathloss exponent (i.e., the type of environment) has a major impact on the gain of the communication link, but not very much on the shape of the correlation function. Figure 5 also reveals that the exponential distribution shows more realistic characteristics for being used in wireless MIMO models.

V. CONCLUSIONS

In this paper, we have proposed a simple, closed-form, and tractable expression for the cross-correlation function of a MIMO channel in an isotropic scattering environment as an extension of the Jakes/Clarke model. Using the novel suggested method of modeling, called free-geometry scatterers, we showed that we are able to consider the appropriate spatial distribution for the local scatterers. As an example in this paper, we considered uniformly distributed scatterers around the MS and the BS. Hence, this method gives us the flexibility to characterize different propagation environments: microcell or macrocell, flat-fading or frequency-selective. In fact, this delay-gain expression, along with the appropriate statistical distributions for the time-delay and the angle spread, plays the role of the geometry of scatterers in the modeling procedure. The correlation function is decomposed into two Bessel functions and other multiplicative terms. Bessel functions represent the Doppler effect, the carrier frequencies and the spatial separation either at the transmitter or at the receiver. The effect of the carrier frequencies also appears on the other terms. The third and fourth terms are $\eta/2$ -order derivative of the moment generating function of the delay profile of the propagating waves evaluated at two carrier frequencies, where η is the environment pathloss exponent. Overall, the model, which is a function of time, space, and frequency, is efficient and accurate for both analytical analysis and simulation purposes. This closed form can be used effectively for simulation, analysis, and design of communication systems over complex MIMO propagation media. This model is easy to understand and could be used for advanced educational objectives. A 3-D extension of this model is presented in [6], employing a realistic elevation angle distribution.

REFERENCES

- [1] D.-S. Shiu, G. J. Foschini, M. J. Gans and J. M. Kahn, "Fading correlation and its effect on the capacity of multielement antenna systems," *IEEE Transactions on Communications*, vol. 48(3), pp. 502-513, March 2000.
- [2] A. Abdi and M. Kaveh, "A Space-Time Correlation Model for Multielement Antenna Systems in Mobile Fading Channels," *IEEE Journal on Selected Areas in Communications*, vol. 20, no. 3, pp. 550-560, April 2002.

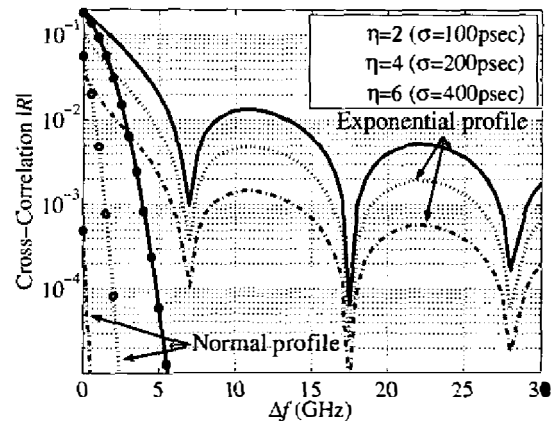


Fig. 5. **Effect of the Environment; Pathloss Exponent:** The cross-correlation function with respect to carrier frequency offset, $\Delta f \triangleq f_2 - f_1$, for different pathloss exponents, η , and delay profiles with mean, $\bar{\tau} = 2\mu\text{sec}$, and different time-delay variances, σ . $f_1 = 1\text{GHz}$, $t_1 = t_2 = 0$ sec, the mobile speed, $V = 50\text{Km/h}$, $M_m = 2(1-j)\text{cm}$, $M_n = (1+j)\text{cm}$, $B_p = 15\text{cm}$, $B_q = 0\text{cm}$. Curves for normal delay profile are circled.

- [3] M. Kalkan and R. H. Clarke, "Prediction of the Space-Frequency Correlation Function for Base Station Diversity Reception," *IEEE Transactions on Vehicular Technology*, vol. 46, no. 1, pp. 176-184, Feb. 1997.
- [4] T. Chen, M. P. Fitz, W. Kuo, M. D. Zoltowski and J. H. Grinn, "A space-time model for frequency nonselective Rayleigh fading channels with applications to space-time modems," *IEEE Journal on Selected Areas in Communications*, vol. 18, no. 7, pp. 1175-1190, July 2000.
- [5] M. Stege, J. Jeltto, M. Bronzel and G. Fettweis, "A Multiple Input - Multiple Output Channel Model for Simulation of Tx and Rx Diversity Wireless Systems," *52nd IEEE Conference on Vehicular Technology*, vol. 2, pp. 833-839, 2000.
- [6] H. S. Rad and S. Gazor, "A three-dimensional Multi-Input Multi-Output Wireless Channel Model," under preparation for submission to *IEEE Transactions on Wireless Communications*, August 2003.
- [7] R. H. Clarke, "A Statistical Theory of Mobile Radio Reception," *Bell Sys. Tech. J.*, pp. 957-1000, July-August 1968.
- [8] T. Svantesson, *Antennas and Propagation from a Signal Processing Perspective*. Ph.D. Dissertation, Department of Signals and Systems, School of Electrical and Computer Engineering, Chalmers University of Technology, Sweden, 2001.
- [9] C. Xiao, Y. R. Zheng and N. C. Beaulieu, "Second-order statistical properties of the WSS Jakes' fading channel simulator," *IEEE Transactions on Communications*, vol. 50, no. 6, pp. 888-891, June 2002.
- [10] M. F. Pop and N. C. Beaulieu, "Limitations of sum-of-sinusoids fading channel simulators," *IEEE Transactions on Communications*, vol. 49, no. 4, pp. 699-708, April 2001.
- [11] H. Nikookar and H. Hashemi, "Phase modeling of indoor radio propagation channels," *IEEE Transactions on Vehicular Technology*, vol. 49, no. 2, pp. 594-606, Mar 2000.
- [12] H. Hashemi and D. Thott, "Statistical modeling and simulation of the RMS delay spread of indoor radio propagation channels," *IEEE Transactions on Vehicular Technology*, vol. 43, no. 1, pp. 110-120, February 1994.
- [13] G. Durgin, *Space-Time Wireless Channels*, NJ: Prentice Hall, 2003.
- [14] T. Rappaport, *Wireless Communications - Principles and Practice*, Prentice Hall PTR, 1994.
- [15] W. C. Jakes, Ed., *Microwave Mobile Communications*, New York: Wiley, 1974.
- [16] A. Papoulis, and S. U. Pillai, *Probability, Random Variables, and Stochastic Processes*, 4th Edition, McGraw-Hill, 2002.
- [17] S. Saunders, *Antennas and Propagation for Wireless Communication Systems*, New York: Wiley, 1999.
- [18] H. L. Bertoni, *Radio Propagation for Modern Wireless Systems*, Prentice Hall PTR, 1999.